International Journal of
INTELLIGENT SYSTEMS AND APPLICATIONS IN ENGINEERING
ISSN:2147-6799 www.ijisae.org Original Research Paper

Object Detection from Satellite Images Employing Ostu-Entropy Segmentation and Deep Neural Networks

Mr. Nishant Vijayvergiya[1], Dr. Rajat Bhandari [2], Dr. Sudhir Agrawal[3]

Submitted: 25/11/2023 **Revised**: 05/01/2024 **Accepted**: 15/01/2024

Abstract: Satellite images have extremely important applications in the domain of remote sensing, security, military, climate monitoring, disaster management etc. One of the key aspects of satellite image analysis happens to be object detection of satellite images which allows to access the context of the image and renders significant information. However, due to the enormous distance from which the image is captured, as well as noise and blurring effects, its is extremely difficult to attain high accuracy of object detection in case of satellite images. This paper presents a method to enhance the quality of satellite images through pre-processing prior to analysis using machine learning algorithms. Different noise categories affecting satellite images have been investigated and an iterative denoising approach has been developed for denoising. Further, a deep neural network model has been developed to identify objects from satellite images. It is shown that the proposed approach attains a classification accuracy of 92.243%, recall of 91.23%, specificity of 91.98%, precision of 90.943% and F-measure of 91.588% outperforming contemporary approaches in the domain.

Keywords: *Satellite image detection, remote sensing, image enhancement, image denoising, deep neural networks, classification accuracy.*

1. Introduction

Modern remote sensing relies heavily on satellite image transmission to link the vast reaches of Earth to global information hubs [1]. High-resolution satellite photos can be sent with ease thanks to these advanced technologies, which opens up a variety of uses for urban planning, disaster relief, and environmental monitoring. Satellite photography is sent to ground stations via a variety of communication channels, such as data transfer protocols and radio frequency signals, by orbiting satellites outfitted with cutting-edge sensors. These communication systems' dependability and efficiency are essential for prompt access to vital information, supporting decision-makers across a range of industries [2]. Whether tracking land cover changes, evaluating agricultural practices, or responding to natural disasters, the capacity to quickly and securely communicate satellite images expands our knowledge of the earth and facilitates well-informed global decision-making [3]. The satellite communication architecture is of fundamental importance in understanding the data transmission model of satellite images [4].

The major blocks of the satellite communication architecture are discussed subsequently. The architecture of satellite communication is made up of an intricate connection of parts and mechanisms intended to make it easier to send data across great distances using satellites in Earth's orbit. This architecture consists of a number of essential components, each of which is vital to maintaining effective and dependable communication [6].

Ground Stations: Strategically positioned on Earth's surface, ground stations form the cornerstone of satellite communication architecture. Large antennas are used by these stations to transmit and receive signals to and from satellites. Data transport is

managed by ground stations, which act as an interface between satellite systems and terrestrial communication networks [7]

Space Segment: The space segment consists of the actual satellites as well as any related subsystems including antennas, power systems, and transponders. Through the reception, amplification, and retransmission of signals from the ground stations back to Earth, the transponders are essential to the communication process. These components are made to endure the hostile environment of orbit and guarantee the satellite's continued operation [8].

Satellite: Satellites orbiting the Earth in various configurations such as geostationary or low Earth orbit. Geostationary satellites remain fixed over a specific point on the Earth's surface, enabling continuous communication with fixed ground stations. Low Earth orbit satellites, on the other hand, move rapidly but offer lower latency. Satellites are equipped with transponders, amplifiers, and antennas to receive, amplify, and retransmit signals [9]

Control Segment: A control segment is necessary in the architecture of satellite communication in order to oversee and manage the satellite fleet. Ground-based control centres in charge of payload management, satellite trajectory

[1] *Research Scholar, SAGE University, Indore, (M.P.), India*
[2] *Research Supervisor, SAGE University, Indore, (M.P.), India.*
[3] *Research Co-Supervisor, SAGE University, Indore, (M.P.), India.*
E-mail Id: [1]nishant.vijay23@gmail.com
[2]2006.bhandari@gmail.com, [3]sudhiragrawal2.1309@gmail.com
** Corresponding Author: Mr. Nishant Vijayvergiya*
Email: nishant.vijay23@gmail.com

control, and overall system health monitoring are included in this section. To make sure the satellites stay in their assigned orbits and operate within predetermined bounds, operators utilise telemetry, tracking, and command (TT&C) systems to connect with the spacecraft [10].

User Terminal: User terminals are the endpoint devices that people, corporations, or organisations use to access satellite communication services. Satellite phones, VSAT (Very Small Aperture Terminal) systems, and other ground-based devices are examples of these terminals. As the conduit between end users and the satellite communication network, user terminals send and receive signals to and from the satellites [11].

Satellite Uplink: As the transmission line from a ground-based Earth station to the satellite in orbit, the uplink is an essential part of the architecture of satellite communication. During this process, the user's terminal sends data, audio, or other information, usually via the antenna of a ground station. The signal ascends through Earth's atmosphere until it reaches the transponder on the satellite, which picks it up, amplifies it, and sends it back to Earth. In order to establish communication links with satellites and deliver data for broadcast or relay, uplink transmissions are necessary [12].

Satellite Downlink: On the other hand, the transmission path from the satellite to the Earth station located on Earth is referred to as the downlink. After receiving the uplink signal, the satellite uses its transponders to process and amplify the data before sending it back to Earth [13]. After being received by the antenna of a ground station, the downlink signal is disseminated to end users or incorporated into terrestrial communication networks for additional processing. In order to complete the two-way communication link and convey information from satellites to users on the ground, downlink broadcasts are essential [14].

Transponders: Important components of the uplink and downlink procedures are satellite transponders. During the downlink, these electronic equipment retransmit the signals they received from the uplink on a different frequency. Transponders allow numerous signals to be broadcast simultaneously without interference in addition to amplifying the signals. In order to prevent signal collisions and effectively handle communication traffic between the satellite and Earth stations, they are set up with designated frequency bands [15].

The satellite communication architecture is depicted in figure 1

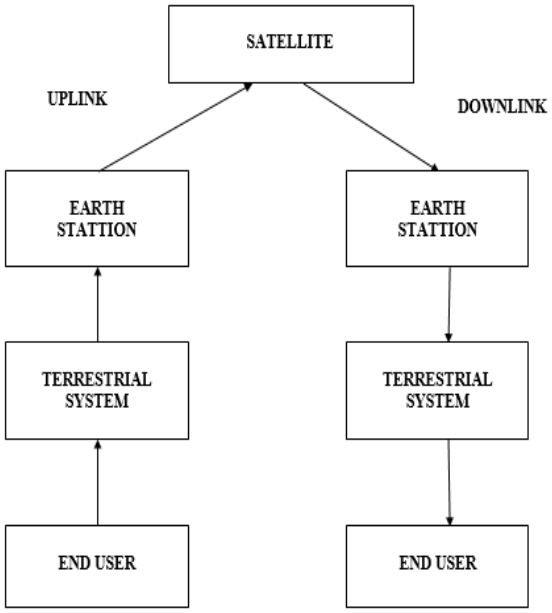

Fig.1 The satellite communication architecture

The next section discusses the importance and salient features of satellite imagery.

2. Satellite Imagery

Innovations in satellite image transmission are helping us monitor and manage Earth's resources and ecosystems more effectively as technology develops. High-resolution imagery of a variety of landscapes, from populated areas to isolated areas, are captured by satellites circling the earth, yielding a plethora of geospatial data. In industries like urban planning, agriculture, disaster relief, and environmental monitoring, these photos play a vital role. Large datasets are sent efficiently and securely through complex technologies and protocols used in the communication infrastructure enabling satellite picture transmission. In addition to providing real-time surveillance, satellite imagery forms the basis for extensive regional studies. Our knowledge of the dynamic Earth system is greatly enhanced by satellite image transmission, which is used for anything from monitoring changes in land cover to evaluating the effects of natural disasters [16]. As communication protocols and satellite technology continue to evolve, the world community can obtain useful insights from these complex visual information more quickly. Typically, the complexity of the satellite images arises out of the capturing mechanism as well as the inherent noise and disturbance in capturing, which make accurate object or context detection challenging [17]..

Fig.2 Example of a satellite image

There are many different kinds of satellite pictures, and each has a distinct function in Earth observation. Optical images, such as Shortwave Infrared (SWIR) and Visible and Near-Infrared (VNIR), are useful for environmental monitoring and land cover categorization. For uses like terrain mapping, radar images—especially Synthetic Aperture Radar (SAR)—offer all-weather capability. Applications like urban heat island monitoring benefit from the measurement of temperature fluctuations provided by infrared pictures, such as Thermal Infrared (TIR). Hyperspectral and multispectral photos combine information from several spectral bands to present a full picture. While stereo photos help create 3D models, panchromatic images improve spatial resolution. Further insights into Earth's properties may be gained via topographic maps, views of the seas and atmosphere, and photos of evening lights. These photos support a variety of disciplines, such as urban planning, agriculture, disaster relief, and climate studies. Advances in satellite technology continue to broaden the range and quality of available imagery [18].

2.1 Salient features of Satellite Images

A variety of characteristics come together to form satellite image communication, which makes it possible to transfer important visual data from orbiting satellites to Earth-based receivers in an effective and dependable manner. The capacity to send photos across great distances, getting over geographical restrictions and offering a worldwide view, is one important advantage. Large datasets may be exchanged securely and seamlessly thanks to the communication infrastructure enabling satellite picture transmission, which is outfitted with strong data transfer protocols. This is especially important for applications that need to monitor things in real time and share information quickly. Furthermore, satellite communication systems may adjust to different frequency bands, providing flexibility in data transfer according to the particulars of the pictures being transmitted [19]..

Another significant characteristic is the capacity to transmit through various weather conditions, including cloud cover, which guarantees uninterrupted data transmission even in the face of atmospheric disturbances. In addition, security issues are addressed by using encryption and authentication systems to protect the confidentiality and integrity of the pictures that are transferred. These characteristics together support the dependability and efficiency of satellite picture transmission in a variety of applications, including scientific research, environmental monitoring, and disaster response, as satellite communication technologies continue to progress [20]..

2.2 Challenges Associated with Satellite Imagery

Satellite image detection faces several challenges, reflecting the complexity of processing and interpreting vast amounts of diverse and high-dimensional spatial data. Some of the existing challenges include [21]:

Data Quality and Availability:

Limited Labelled Data: It might be difficult to find labelled datasets for deep learning model training, particularly for uncommon and specialised classes. Inadequate data could make it more difficult for the model to generalise.

Data heterogeneity: The consistency and calibre of satellite images can be impacted by differences in picture resolution, sensor attributes, and atmospheric circumstances.

Computational Resources:

High Computational Demands: Significant computational resources are required for training deep neural networks, especially when working with huge datasets. For certain researchers and organisations, access to strong computer infrastructure could be a limitation.

Interclass Variability:

Difficult Land Cover Types: The surface of the Earth displays a variety of complex land cover types and complicated patterns. It has always been difficult to create models that can discriminate between complicated classes with minute spectral deviations [22].

Time and Space Variability:

Dynamic Environments: Weather fluctuations, seasonal variations, and temporal dynamics all pose difficulties for monitoring and detection, particularly when using static models that could find it difficult to adjust to changing circumstances.

Generalisation and Transferability*:*

Transfer Learning Challenges: Because different land cover types exist in different geographic locations, it can be difficult to adapt models trained in one place to another. Generalizing models across diverse settings remains a challenge.

Semantic Gap: Semantic Understanding: It's still difficult to create models that comprehend situations more deeply than just pixel-by-pixel identification, including item connections and context.

Interference and Noise: Atmospheric Conditions: The quality of data and the effectiveness of detection algorithms can be negatively impacted by cloud cover and atmospheric interference, which can obfuscate satellite pictures.

Sensor Noise: Differences in sensor properties can cause noise, which reduces the precision of image detection algorithms [23].

Real-Time Processing:

Operational Latency: Algorithms that may have high computing demands and may not be appropriate for quick, on-the-spot analysis may have difficulties in some applications that call for real-time or almost real-time processing.

To tackle these issues, multidisciplinary approaches are needed, including developments in machine learning algorithms, technology for remote sensing, data standardisation, and cooperative projects to provide extensive and varied datasets for training and assessment. Overcoming these obstacles will help satellite image detection applications become more widely used and more successful as technology and approaches advance [24].

3. Methodology

The methodology developed in this paper focusses on addressing the inherent limitations in object detection of satellite images along with research gap present in existing literature. The major challenges inherent to satellite imagery are [25]-[26]:

1) Extremely large distance of the satellite from the earth with the atmospheric envelope resulting in considerable refraction.

2) Variation in material constants in the atmospheres such as the relative permittivity (ε_r), permeability (μ_r) and conductivity (σ) causing variations in EM wave characteristics resulting in image distortions.

3) Blurring, noise and degradation effects resulting out of electronic noise (Gaussian), sudden spikes in equipment currents and voltages (salt and pepper), multiplicative additions to image pixels (Speckle) and inadequacy of captured pixels to recreate image (Poisson).

4) Blurring effects in images limiting the process of segmentation and masking of captured images.

The machine learning and deep learning limitations often emanate from potential overfitting of deep learning models to the vanishing gradient problem. Moreover, imbalanced datasets in certain categories of satellite images render inaccuracies in classification. The extreme variability in satellite image datasets in terms of capturing time, incident lighting, atmospheric characteristics and type of objects being captured may lead to inaccuracies to deep learning models as the feature extraction mechanism of an architecture takes away the control of feature selection.

To address the aforesaid issues, this paper proposes a two fold approach which entails image pre-processing prior to a machine learning based approach for identification/ classification.

3.1 Contrast Enhancement

Contrast enhancement plays a key role in the subsequent segmentation process and final classification. Typically, the background enhancement is based on the improvement of image contrast as one of the most important statistical features of the image. The contrast of an image $I(i,j)$ is computed as [27]:

$$\boldsymbol{Contrast} = \sqrt{\frac{1}{mn}\sum_{i,j}^{m,n}[\boldsymbol{X}(\boldsymbol{i},\boldsymbol{j}) - \boldsymbol{Mean}(\boldsymbol{i},\boldsymbol{j})]^2} \quad \textbf{(1)}$$

Here,

X denotes the original image.

(i,j) denote the pixels.

$Mean$ denotes the average value of the pixels

The contrast enhancement process, the statistical dissimilarity between the actual Region of Interest (ROI) and the background is maximized, thereby increasing the contrast of the image. This is done by maximizing the standard deviation of the mean pixel values through a cost function defined as:

Algorithm*:*

{

$\boldsymbol{for}\ (\boldsymbol{i} = \boldsymbol{1}{:}\,\boldsymbol{m})\ \&\ (\boldsymbol{j} = \boldsymbol{1}{:}\,\boldsymbol{n})$

$\boldsymbol{maximize}\ (\boldsymbol{C_\sigma} = \sqrt{\frac{1}{N}\sum_{i}^{N}(\boldsymbol{X_i} - \boldsymbol{\mu})^2}\ )$

And

$\boldsymbol{minimize}\ (\boldsymbol{C_{corr}} = \sum_{i,j}^{m,n}\frac{(i-u_x)(j-\mu_j)P_{j_{x,y}}}{\sigma_x\sigma_y})$

}

Here,

C_σ denotes the standard deviation of based Cost Function.

C_{corr} denotes the correlation among pixel patches.

The idea here is to simultaneously enhance the contrast difference by maximizing the standard deviation among the ROI and background and minimizing the cross-correlation among the ROI and background.

The subsequent step is the illumination correction applied to satellite images based on a Gaussian Kernel function. The illumination correction reduces the probability of false contour identification due to variability in captured pixel intensity. In this approach, a Gaussian Kernel Function is used for illumination correction as it is effective in normalizing the dynamic range of the image intensities, and is mathematically expressed as [28]:

$$\boldsymbol{G(x,y) = ke^{\frac{-(x^2+y^2)}{s^2}}} \quad \textbf{(2)}$$

Here,

$\boldsymbol{G(x,y)}$is the Gaussian Kernel.

$\boldsymbol{k}$represents the normalizing co-efficient.

$\boldsymbol{s}$represents the scaling co-efficient of the kernel.

$(\boldsymbol{x,y})$represent the spatial co-ordinates.

The reflection co-efficient value $I_R(x,y)$ is estimated by convolving the input image and the Gaussian function in the periphery bound the contour $'C'$. The weight co-efficient $\boldsymbol{w}$is updated throughout the contour for the number of scales $\boldsymbol{i = 1:n}$. Further a linear transform to adjust the objectively captured image I and the corrected image I_C is expressed as:

$$\boldsymbol{I_C = \beta_1 log_e I + \beta_2} \quad \textbf{(3)}$$

Here,

I and I_C corresponds to the physically captured and illumination corrected images respectively.

$\boldsymbol{\beta_1\ and\ \beta_2}$are correction constants].

The next process is the computation of the two-dimensional spatial correlation given by:

$$\boldsymbol{C(x,y) = \frac{I(x,y)-I_C(x,y)}{I(x,y)-I_B(x,y)}.k} \quad \textbf{(4)}$$

Here,

C represents the correlation.

k denotes the normalizing co-efficient.

I denotes the original image

I_C denotes image correlation

I_B denotes image background

The histogram normalization is computed based on the difference in the Eigen values of the original and corrected image given by:

$$\boldsymbol{|kI - I_C|} \quad \textbf{(6)}$$

The covariance of the image can be computed using:

$$\boldsymbol{C_V = \frac{mean\,[I(x,y)-I_C(x,y)]}{|kI-I_C|}} \quad \textbf{(7)}$$

Here,

$mean$ denotes the average operation.

The subsequent process is to add the product of the weight matrix and normalized co-variance co-efficient to the originally corrected image:

$$\boldsymbol{N_I = I(x,y) - I_C\{(x,y)\} + mean(w * C_V)]} \quad \textbf{(8)}$$

Here,

N_I denotes the normalized image.

w denotes the correlation weights.

3.2 Segmentation and Masking

Contrary to the segmentation process for relatively regular shapes exhibiting smooth changes in pixel boundaries, satellite images often exhibit extremely variability in pixel boundaries making the computation of the conventional radial gradient infeasible. This paper presents a hybrid entropy based Ostu segmentation process. Primarily, the gradient maximizing function is computed as:

$$\boldsymbol{g = Max[E(\frac{\partial}{\partial r}\oint_{x_i}^{x_f}\frac{I(x,y)}{\mu(i,j)}ds|)]} \quad \textbf{(9)}$$

Here,

E denotes the entropy of the closed region given by:

$$\boldsymbol{E = -P(I_{i,j})log_2 I_{i,j}} \quad \textbf{(10)}$$

Max denotes the maximizing operation.

$\frac{\partial}{\partial r}$ denotes the radial gradient over the closed contour 'S'

ds denotes the differential area.

$\mu(i,j)$ denotes the mean pixel value.

The idea here is to maximize the average information (Entropy) of the segmented region within the closed contour for segmentation 'R'. This hybrid approach combines both the adaptive Ostu thresholding as well as an entropy based segmentation (probabilistic segmentation) so as to effectively separate out the region of interest not only based on pixel statistics but also based on region wise information statistics [29].

The masking is done to the ROI of effected patches, for which the pixel correlation is computed for a patch of images wherein the segmentation is to be applied and is expressed as:

$$\boldsymbol{C_{patch} = \|P_T - P_C\|^2} \quad \textbf{(11)}$$

Here,

$\boldsymbol{C_{patch}}$denotes the squared Euclidean norm for the patch.

$\boldsymbol{P_T}$denotes the target patch.

$\boldsymbol{P_T}$denotes the candidate patch.

Next, the pixels are weighed averages of the existing pixels satisfying the interpolation condition given by:

$$\boldsymbol{Z = argmin(P_T - P_C) \ll mean|P_S|} \quad \textbf{(12)}$$

Here,

Z is the minimum interpolated difference co-efficient.

$\boldsymbol{mean|P_S|}$is the average pixel magnitude of the patch.

Thus the pest infested patch for segmentation and remaining part to be fused can be done using the consecutive standard deviations given by:

$$\boldsymbol{\mu + \frac{\sigma^2}{(\sigma+1)^2}} \quad \textbf{(13)}$$

Here,

μ is the average pixel values.

σ is the standard deviation.

3.3 Object Identification:

The final step is to design a neural network model for identification of the particular object or context from the composite image. While there are several machine learning and deep learning based approaches for object detection, most of the approaches in the context of satellite image identification face the challenge of imbalanced datasets and high variability among pixel characteristics. This approach presents a deep neural network based approach employing the Baye's probabilistic optimization. In case the training vector contains K samples, $(f^1 \ldots . f^K)$ and corresponding weights to them, $(W^1 \ldots . W^K)$, the weighted centres of the positive and negative samples in the complete feature space can be computed as:

$$\boldsymbol{Center_W^P = \frac{1}{|P|}\sum_{F\epsilon P} W(f).f} \quad \textbf{(14)}$$

$$\boldsymbol{Center_W^N = \frac{1}{|N|}\sum_{F\epsilon N} W(f).f} \quad \textbf{(15)}$$

The in class and within class scatter variance metrics can be computed as:

$$V_I = \boldsymbol{(Center_W^P - Center_W^N).(Center_W^P - Center_W^N)^T} \quad \textbf{(16)}$$

$$\boldsymbol{V_W = \sum_{F\epsilon P} W(f).(F - Center_W^P)(F - Center_W^P)^T + \sum_{F\epsilon N} W(f).(F - Center_W^N)(F - Center_W^N)^T} \quad \textbf{(17)}$$

The projection vector $\boldsymbol{p}$ can be iteratively updated to generated feature combinations (which can discriminate among classes) based on the condition given as

$$\boldsymbol{p = arg\ max\ (J(w) = agr\ max\ \frac{w^T V_W . w}{w^T V_I . w}}$$ **(18)**

Optimizing equation (18) generates the best feature combinations employing the penalty factor given by:

The penalty factor is defined as $\boldsymbol{\rho = \frac{\mu}{v}}$ and is used to update the weights of the networks such that the modified regularized cost function:

$$\boldsymbol{F(w) = \mu w^T w + v[\frac{1}{n}\sum_{i=1}^{n}(p_i - a_i)^2]}$$ **attains a minima, (19)**

If $(\mu \ll v)$: Network error are generally low.

else if $(\mu \geq v)$: Network errors tend to increase, in which case the weight magnitude should be reduced so as to limit errors **(Penalty)** [31].

The proposed algorithm is presented next.

Proposed Algorithm:

Start

{

Step.1 Split data into training and testing samples in the ratio of 70:30.

Step.2: Apply Contrast Enhancement based on:

$$\boldsymbol{for\ (i = 1{:}m)\ \&\ (j = 1{:}n)}$$

$$\boldsymbol{maximize\ (C_\sigma = \sqrt{\frac{1}{N}\sum_i^N (X_i - \mu)^2}\ )}$$

$$\boldsymbol{and}$$

$$\boldsymbol{minimize\ (C_{corr} = \sum_{i,j}^{m,n} \frac{(i-u_x)(j-\mu_j)P_{j_{x,y}}}{\sigma_x \sigma_y})}$$

}

Step.3: Based on the Gaussian Kernel function, compute the 2-D pixel correlation as:

$$\boldsymbol{C(x,y) = \frac{I(x,y) - I_C(x,y)}{I(x,y) - I_B(x,y)}.k}$$

Step.4 Obtain normalized image as:

$$\boldsymbol{N_I = I(x,y) - I_C\{(x,y)\} + mean(w * C_V)]}$$

Step.5: Apply segmentation based on the Entropy-Ostu hybrid approach as:

$$\boldsymbol{g = Max[E(\frac{\partial}{\partial r}\oint_{x_i}^{x_f} \frac{I(x,y)}{\mu(i,j)} ds|)]}$$

Step.6: Mask image based on the condition:

$$\boldsymbol{Z = argmin(P_T - P_C) \ll mean|P_S|}$$

Step.7: Defined cost function and set tolerance as:

$$\boldsymbol{C = \frac{1}{n}\sum_{i=1}^{n}(pred_1 - y_i)^2}$$

$$\boldsymbol{C_{tolerance} = 1e^{-6}}$$

Step.8 $\boldsymbol{(for\ 1{:}\ max\ iterations)}$***,***

Optimze:

$$p = arg\ max\ (J(w) = agr\ max\ \frac{w^T V_W . w}{w^T V_I . w}$$

And

$$F(w) = \mu w^T w + v[\frac{1}{n}\sum_{i=1}^{n}(p_i - a_i)^2$$

$$if\ i =$$
$$= max\ iterations\ or\ C\ statbilizes\ in\ tolerance$$

Stop training

$$else\ (iterate\ over\ steps\ 7\ and\ 9$$

$$end\ if.$$

}

Stop.

4. Experimental Results

The experiment is conducted on the benchmark TGRS-HRRSD, DOTA-v1.5 and RSOD datasets. The data is split randomly in the ratio of 70:30. The number of image for testing for the 3 datasets are 900, 700 and 1000 for the 3 datasets respectively.The simulation has been conducted on Matlab 2022a on a PC with an Intel i5-9300H CPU with NVIDIA GeForce GTX 1650 GPU. The simulation results are presented next:

Fig.3 Original Image

Fig.4 Illumination Correction

Fig.5 Grayscale Image

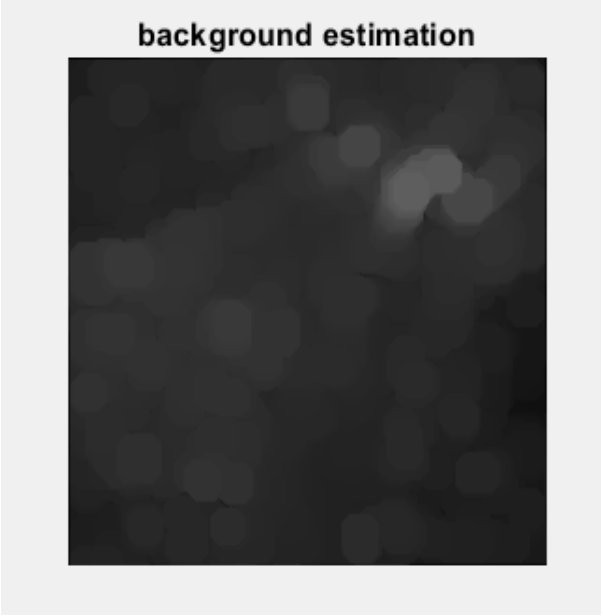

Fig.6 Background Estimation

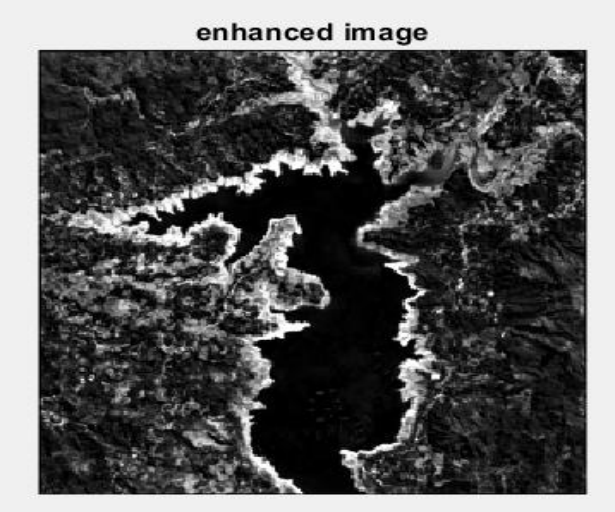

Fig.7 Contrast Enhanced Image

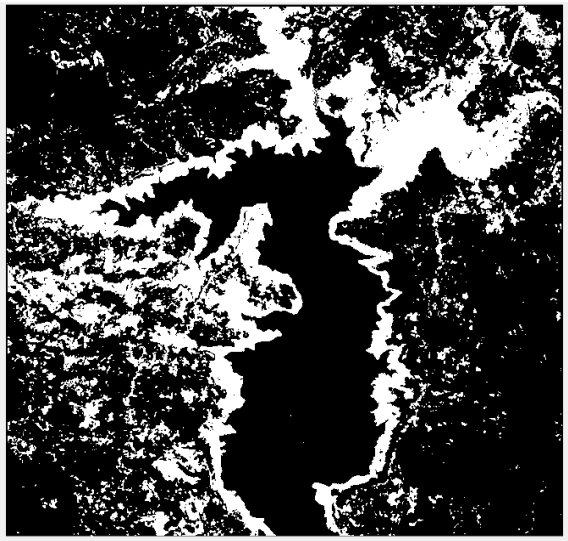

Fig.8 Thresholding at 30%

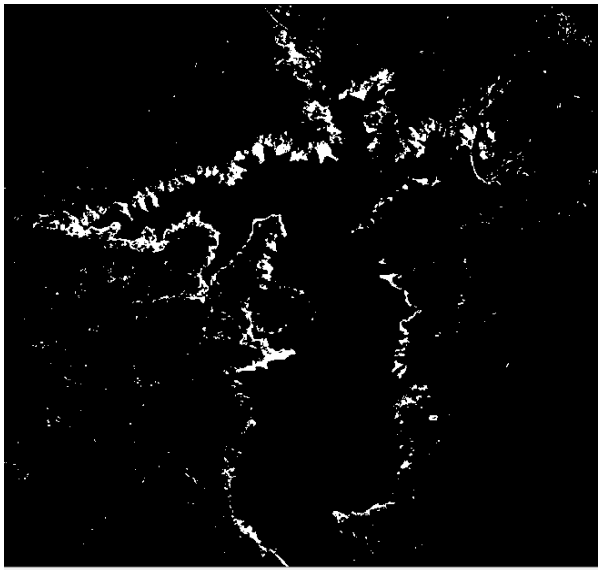

Fig.9 Thresholding at 60%

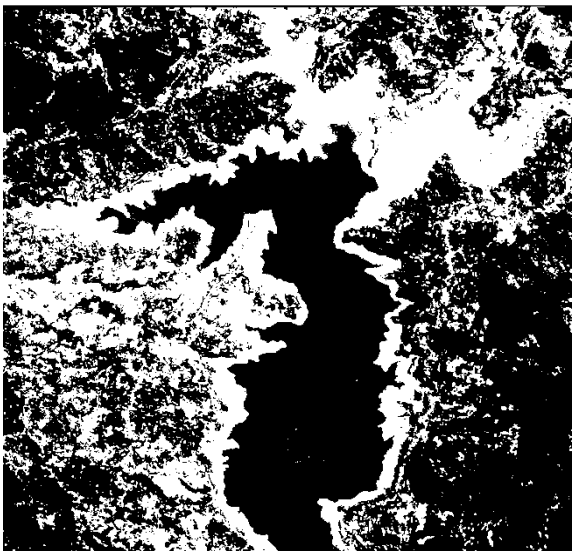

Fig.10 Hybrid Ostu-Entropy Segmentation

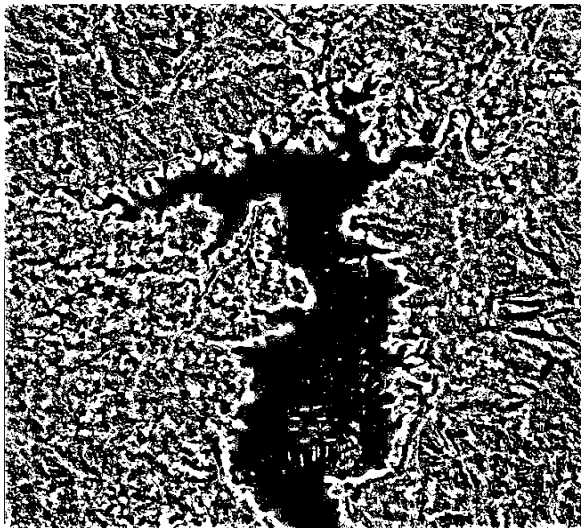

Fig.11 Segmentation Inversion

Fig.12 Masking

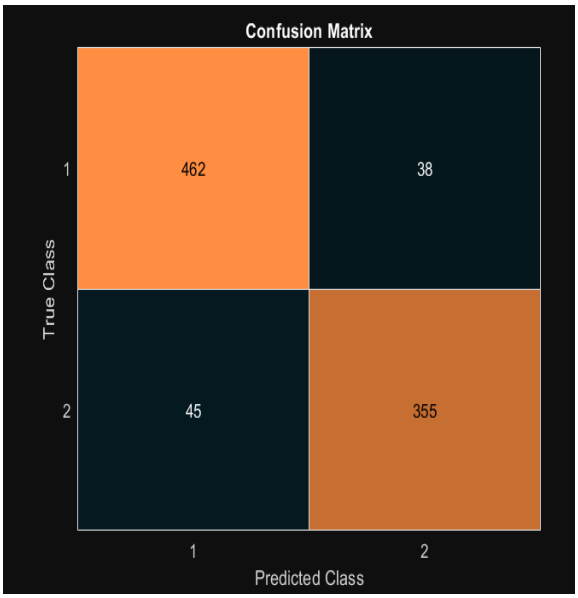

Fig,13 Confusion Matrix for Dataset-1

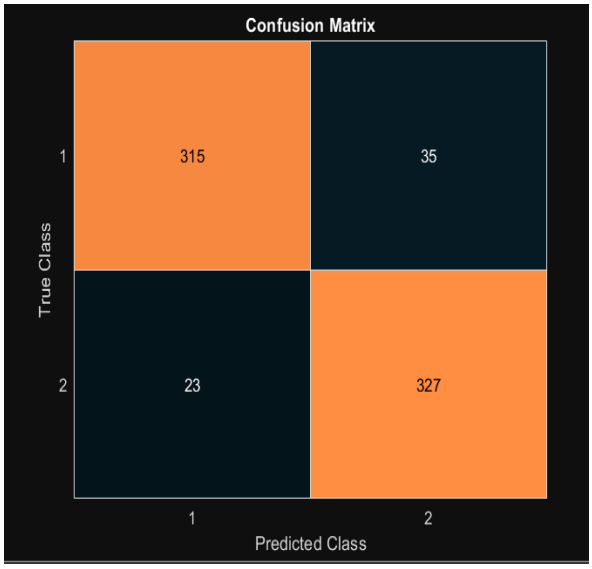

Fig,14 Confusion Matrix for Dataset-2

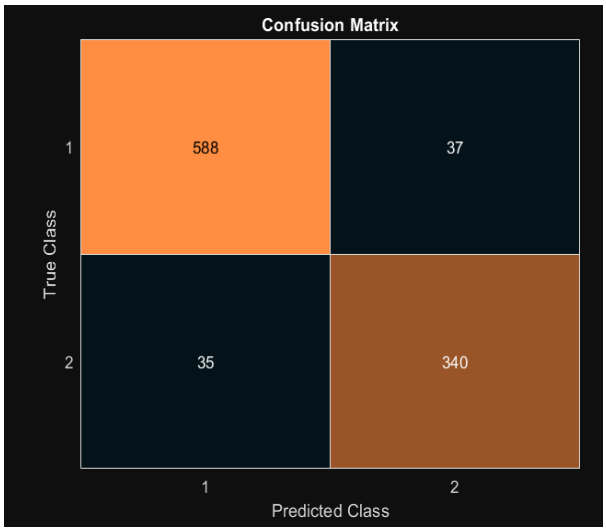

Fig,15 Confusion Matrix for Dataset-3

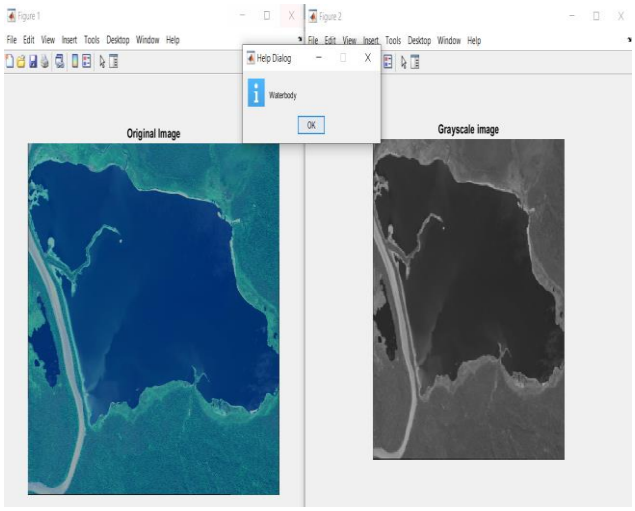

Fig.16 Detection of Water Body

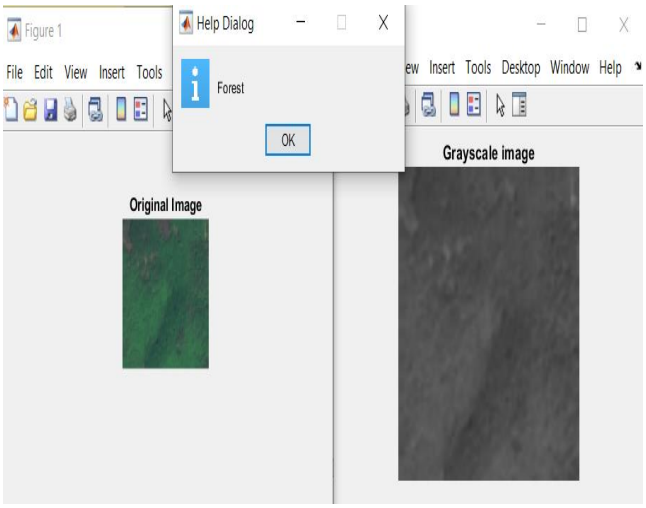

Fig.17 Detection of Forest

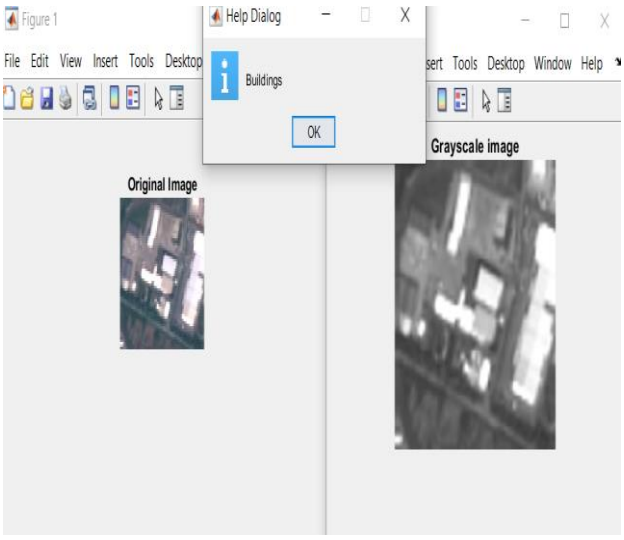

Fig.18 Detection of Buildings

Discussions:

This paper presents a rigorous image-pre processing mechanism based on contrast enhancement, illumination equalization and Entropy-Ostu segmentation and masking. Figure 3 presents the original RGB image and figure 4 presents its illumination corrected counterpart. Figure 5 presents the grayscale version of the image. Figure 6 presents the contrast enhanced image.

Figure 7 and 8 depict the thresholding process prior segmentation at 30% and 60% threshold values. It can be observed from the images that while 30% threshold incorporates more background objects, 60% threshold eliminates several details of the boundary. Hence, a need for an optimal segmentation approach is needed which is presented in figure 9, in terms of the Entropy-Ostu hybrid proposed in this paper. An invertible segmentation of the method is presented in figure 10, which can alternatively used in case the background is to be identified instead of the conventional ROI in the image. Figure 12 depicts the masking of the image.

Figures 13, 14 and 15 depicts the confusion matrix for the 3 datasets respectively. The confusion matrix gives us the values of true positive (TP), true negative (TN), false positive (FP) and false negative (FN) respectively. These metrics allow us to compute the following performance metrics:

Accuracy:

$$Ac = \frac{TP+TN}{TP+TN+FP+FN} \quad (20)$$

Sensitivity/Recall:

$$Se\ or\ Re = \frac{TP}{TP+FN} \quad (21)$$

Precision:

$$Pr = \frac{TP}{TP+FP} \quad (22)$$

Specificity:

$$Sp = \frac{TN}{TN+FP} \quad (23)$$

The F-measure is computed as:

$$F - Measure = 2.\frac{Pr.Re}{Pr+Re} \quad (24)$$

Here,

(TP): True Positive

(TN): True Negative

(FP): False Positive

(FN): False Negative

Table.1 Summary of Obtained Results

Parameter	Accuracy%	Sensitivity Or Recall %	Specificity%	Precision%	F-Measure
Dataset-1	92.22	92.4	91.12	88.75	91.755
Dataset-2	91.71	90.00	93.1	93.42	91.52
Dataset-3	92.8	91.29	91.72	90.66	91.49
Overall	**92.243**	**91.23**	**91.98**	**90.943**	**91.588**

The proposed approach attains a classification accuracy of 92.243%, recall of 91.23%, specificity of 91.98%, precision of 90.943% and F-measure of 91.588% and an average measure across all the 3 datasets. As an illustration, the simple classification for prototype testing is presented in figures 16, 17 and 18 respectively which shows that model classifying new images into categories of waterbody, forest and buildings.

Table.2 Comparison with Previous Work

Authors	Source	Approach	Mean Accuracy %
Yan et al.	MDPI, 2021	Faster R-CNN	75.86
Yang et al.	MDPI, 2022	RS-YOLOX	91.52%
Haryono et al.	Wiley, 2023	ResNeXT	89.41
Laiyay et al.	Springer, 2023	CNN-SVM CNN-RF LinkNet-ResNet	81% 82% 87.4%
Miroszewski et al	IEEE, 2023	Quantum-Kernel Support Vector	91.9%
Proposed Approach		**Ostu-Entropy Segmentation with Deep**	**92.243%**

A comparative analysis with contemporary approaches has been presented w.r.t. noteworthy contribution in the field and is cited in table 2. It can be observed that the conventional approaches typically adopted for satellite

object identification are the variants of the convolutional neural network (CNN) such as YOLO, ResNet, variants of the SVM, and hybrid models such as CNN-SVM, CNN-RF etc. However, the proposed approach outperforms the baseline contemporary approaches in terms of classification accuracy.

5. Conclusion

This paper focusses on developing a technique which can address the challenges inherently associated with satellite object detection. The various types of noise and disturbances along with their causes has been discussed in this paper. The paper focusses on developing a technique which can effectively perform illumination correction and contrast enhancement prior to the segmentation and masking processes. A hybrid entropy-Ostu segmentation technique has been developed in this paper. Contrary to the conventional segmentation processes, this approach combines an entropy based approach along with maximum gradient to separate the image ROI (object) from the background, allowing a more refined separation of the actual ROI compared to the conventional maximal gradient or entropy based segmentation applied alone. The classification is done employing a deep neural network based on Bayes optimization combining optimal features for training, with a reward/penalty for the gradient moving towards/away from convergence in each iteration. This allows for a faster convergence compared to conventional CNN variants such as AlexNet, VGGNet, YOLO etc. by targeting the movement of the maximal gradient along convergence. The overall accuracy of the proposed classification has been shown to be better compared to previously existing contemporary approaches thereby proving the efficacy of the proposed approach.

The future directions of this research may be focused on a separate noise removal mechanism for the satellite images combined with DeepNets.

Author contributions

Mr. Nishant Vijayvergiya: Conceptualization, Methodology, Software, Field study, Data curation, Writing-Original draft preparation, Software, Validation., Field study. **Dr. Rajat Bhandari:** Visualization, Investigation, Writing-Reviewing and Editing. **Dr. Sudhir Agrawal:** Visualization, Investigation, Writing-Reviewing and Editing.

Conflicts of interest

The authors declare no conflicts of interest.

References

[1] J Lindahl, R Johansson, D Lingfors, “Mapping of decentralised photovoltaic and solar thermal systems by remote sensing aerial imagery and deep machine learning for statistic generation”, Energy and AI, Elsevier 2023, vol. 14., 100300.

[2] L. He, J. Shan and D. Aliaga, "Generative Building Feature Estimation From Satellite Images," in IEEE Transactions on Geoscience and Remote Sensing, vol. 61, pp. 1-13, 2023, Art no. 4700613.

[3] M. Zhao, P. Olsen and R. Chandra, "Seeing Through Clouds in Satellite Images," in IEEE Transactions on Geoscience and Remote Sensing, vol. 61, pp. 1-16, 2023, Art no. 4704616.

[4] X. Zhu and C. Jiang, "Integrated Satellite-Terrestrial Networks Toward 6G: Architectures, Applications, and Challenges," in IEEE Internet of Things Journal, 2021, vol. 9, no. 1, pp. 437-461.

[5] D Yang, Y Zhou, W Huang, X Zhou, “5G mobile communication convergence protocol architecture and key technologies in satellite internet of things system”, - Alexandria Engineering Journal, Elsevier 2021, vol.60., no.1., pp. 465-476.

[6] V. S. Chippalkatti, R. C. Biradar and S. S. Rana, "Recent Technology Trends in Satellite Communication Subsystems," 2021 IEEE International Conference on Electronics, Computing and Communication Technologies (CONECCT), Bangalore, India, 2021, pp. 1-5.

[7] H. Al-Hraishawi, H. Chougrani, S. Kisseleff, E. Lagunas and S. Chatzinotas, "A Survey on Nongeostationary Satellite Systems: The Communication Perspective," in IEEE Communications Surveys & Tutorials, vol. 25, no. 1, pp. 101-132, Firstquarter 2023.

[8] O. Kodheli et al., "Satellite Communications in the New Space Era: A Survey and Future Challenges," in IEEE Communications Surveys & Tutorials, vol. 23, no. 1, pp. 70-109, Firstquarter 2021.

[9] D. -H. Na, K. -H. Park, Y. -C. Ko and M. -S. Alouini, "Performance Analysis of Satellite Communication Systems With Randomly Located Ground Users," in IEEE Transactions on Wireless Communications, vol. 21, no. 1, pp. 621-634, Jan. 2022.

[10] F. Davarian et al., "Improving Small Satellite Communications in Deep Space—A Review of the Existing Systems and Technologies With Recommendations for Improvement. Part I: Direct to Earth Links and SmallSat Telecommunications Equipment," in IEEE Aerospace and Electronic Systems Magazine, vol. 35, no. 7, pp. 8-25, 1 July 2020.

[11] A Guidotti, S Cioni, G Colavolpe, M Conti, T Foggi, “Architectures, standardisation, and procedures for 5G Satellite Communications: A survey”, Computer Networks, Elsevier, 2020, vol.183, 107588.

[12] K. -X. Li et al., "Downlink Transmit Design for Massive MIMO LEO Satellite Communications," in IEEE Transactions on Communications, vol. 70, no. 2, pp. 1014-1028, Feb. 2022.

[13] N. Okati, T. Riihonen, D. Korpi, I. Angervuori and R. Wichman, "Downlink Coverage and Rate Analysis of Low Earth Orbit Satellite Constellations Using Stochastic

Geometry," in IEEE Transactions on Communications, vol. 68, no. 8, pp. 5120-5134, Aug. 2020.

[14] B. Al Homssi and A. Al-Hourani, "Optimal Beamwidth and Altitude for Maximal Uplink Coverage in Satellite Networks," in IEEE Wireless Communications Letters, vol. 11, no. 4, pp. 771-775, April 2022.

[15] P. Wach and A. Salado, "Model-Based Requirements (TMBR) of a Satellite TTC Transponder," 2021 IEEE Aerospace Conference (50100), Big Sky, MT, USA, 2021, pp. 1-12.

[16] P. Tang, P. Du, J. Xia, P. Zhang and W. Zhang, "Channel Attention-Based Temporal Convolutional Network for Satellite Image Time Series Classification," in IEEE Geoscience and Remote Sensing Letters, vol. 19, pp. 1-5, 2022, Art no. 8016505.

[17] X. Chen, C. Qiu, W. Guo, A. Yu, X. Tong and M. Schmitt, "Multiscale Feature Learning by Transformer for Building Extraction From Satellite Images," in IEEE Geoscience and Remote Sensing Letters, vol. 19, pp. 1-5, 2022, Art no. 2503605.

[18] M. Gazzea, M. Pacevicius, D. O. Dammann, A. Sapronova, T. M. Lunde and R. Arghandeh, "Automated Power Lines Vegetation Monitoring Using High-Resolution Satellite Imagery," in IEEE Transactions on Power Delivery, vol. 37, no. 1, pp. 308-316, Feb. 2022.

[19] J Wang, M Bretz, MAA Dewan, MA Delavar -, "Machine learning in modelling land-use and land cover-change (LULCC): Current status, challenges and prospects", Science of the Total Environment, Elsevier, 2022., vol.822, 153559.

[20] JG Fernández, S Mehrkanoon, "Broad-UNet: Multi-scale feature learning for nowcasting tasks", Neural Networks, Elsevier, 2021, vol.144, pp. 419-427.

[21] J. Kang, S. Tariq, H. Oh and S. S. Woo, "A Survey of Deep Learning-Based Object Detection Methods and Datasets for Overhead Imagery," in IEEE Access, vol. 10, pp. 20118-20134, 2022.

[22] Q. Ran, Q. Wang, B. Zhao, Y. Wu, S. Pu and Z. Li, "Lightweight Oriented Object Detection Using Multiscale Context and Enhanced Channel Attention in Remote Sensing Images," in IEEE Journal of Selected Topics in Applied Earth Observations and Remote Sensing, vol. 14, pp. 5786-5795, 2021.

[23] W. Han et al., "Methods for Small, Weak Object Detection in Optical High-Resolution Remote Sensing Images: A survey of advances and challenges," in IEEE Geoscience and Remote Sensing Magazine, vol. 9, no. 4, pp. 8-34, Dec. 2021.

[24] ZZ Wu, XF Wang, L Zou, LX Xu, XL Li, T Weise, "Hierarchical object detection for very high-resolution satellite images", Applied Soft Computing, Elsevier 2021, vol.113., Part-A., 107885.

[25] A Singh, A Kumar, A Rani, KK Sharma, "Image Denoising for Satellite Imagery Using Amalgamated ROAD-TGM and PCA Algorithm", Artificial Intelligence and Machine Learning in Satellite Data Processing and Services, Springer 2023, pp 143–150.

[26] V. Alves de Oliveira et al., "Satellite Image Compression and Denoising With Neural Networks," in IEEE Geoscience and Remote Sensing Letters, vol. 19, pp. 1-5, 2022, Art no. 4504105.

[27] W. Zhang, P. Zhuang, H. -H. Sun, G. Li, S. Kwong and C. Li, "Underwater Image Enhancement via Minimal Color Loss and Locally Adaptive Contrast Enhancement," in IEEE Transactions on Image Processing, vol. 31, pp. 3997-4010, 2022.

[28] L Ren, AA Heidari, Z Cai, Q Shao, G Liang, HL Chen, "Gaussian kernel probability-driven slime mould algorithm with new movement mechanism for multi-level image segmentation", Measurement, Elsevier 2022, vol.192., 110884.

[29] J Zhao, M Zhang, Z Mao, C Wang, "Reconstruction of 3D Digital Core of Inter Salt Shale Based on OSTU Segmentation Algorithm Optimized by PSO", Proceedings of the International Field Exploration and Development Conference, Springer 2022 pp 6552–6562.

[30] YJ Joo, SY Kho, DK Kim, HC Park, "A data-driven Bayesian network for probabilistic crash risk assessment of individual driver with traffic violation and crash records", Accident Analysis & Prevention, Elsevier 2022, vol.176, 106790.

[31] D Yan, G Li, X Li, H Zhang, H Lei, K Lu, M Cheng, F Zhu, "An improved faster R-CNN method to detect tailings ponds from high-resolution remote sensing images", Remote Sensing, MDPI, 2021, vol.13, 2052.

[32] L Yang, G Yuan, H Zhou, H Liu, J Chen, H Wu, "RS-Yolox: A high-precision detector for object detection in satellite remote sensing images", Applied Sciences, MDPI, 2022, vol.12., , 8707.

[33] A Haryono, G Jati, W Jatmiko, "Oriented object detection in satellite images using convolutional neural network based on ResNeXt", ETRI Journal , Wiley, pp.1-16.

[34] MY Lilay, GD Taye, "Semantic segmentation model for land cover classification from satellite images in Gambella National Park, Ethiopia", SN Applied Sciences, Springer 2023, vol.5, no.76., pp.1-15.

[35] A. Miroszewski et al., "Detecting Clouds in Multispectral Satellite Images Using Quantum-Kernel Support Vector Machines," in IEEE Journal of Selected Topics in Applied Earth Observations and Remote Sensing, 2023, vol. 16, pp. 7601-7613.